Chapter 5

REMOVAL OF CHROMIUM USING NANO CRYSTALLINE ZIRCONIA

In this chapter, the capability of adsorption of chromium on synthesized nano crystalline zirconia is discussed. The effect of various parameters and their significance on removal (%) of chromium is assessed. The isotherm and kinetic parameter determination by linear and nonlinear curve fitting methods are assessed and reported. Thermodynamic parameters were also determined for evaluation of adsorption feasibility.

5.1. Adsorption experiments

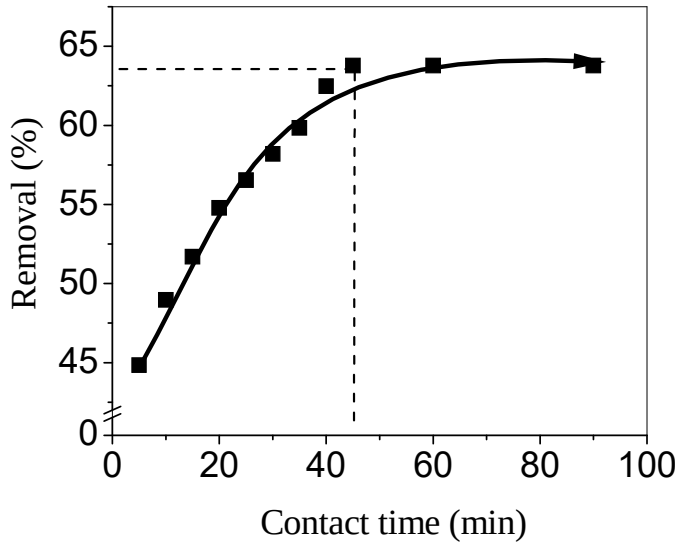

Figure 5.1 Effect of contact time on removal (%) of chromium from aqueous solution on nano crystalline zirconia (initial concentration = 10 mg L^{-1}, pH = 6.6, adsorbent dose = 2 g L^{-1}, agitation speed= 120 rpm temperature = 303K)

Experiments were conducted to assess the time of equilibrium for adsorption of chromium by nano crystalline zirconia and the results are reported in Figure 5.1. A solution of chromium (initial concentration 10 mg L^{-1}) was taken in reagent bottle and 2 g L^{-1} of adsorbent was added to it. The experiments were carried out at 6.6 pH, 120 rpm and at 303 K. It is clear from the Figure 5.1 that initially removal of chromium increased rapidly and then the removal was gradual. It becomes almost constant (ca. 63 %) after 45min. Thus, the equilibrium contact time for the removal of chromium by nanocrystalline zirconia was 45 min.

Table 5.1 Experimental runs for removal of chromium utilizing nano crystalline zirconia

Run order	Initial conc. (mg L^{-1})	pH	Adsorb-ent dose (g L^{-1})	Temp (K)	Removal (%)	Run Order	Initial conc. (mg L^{-1})	pH	Adsorbent dose (g L^{-1})	Temp (K)	Removal (%)
1	35	5.5	6	308	41.67	16	35	5.5	6	308	36.02
2	65	5.5	6	308	33.13	17	5	5.5	6	308	84.21
3	20	8	4	303	17.68	18	35	0.5	6	308	62.31
4	35	5.5	6	308	36.62	19	50	8	4	313	7.80
5	35	5.5	2	308	14.67	20	35	5.5	6	308	39.79
6	35	5.5	6	318	30.79	21	20	3	4	303	75.07
7	50	8	4	303	4.51	22	35	10.5	6	308	4.92
8	50	8	8	313	11.14	23	35	5.5	6	308	36.02
9	50	8	8	303	9.80	24	20	8	4	313	21.26
10	50	3	4	313	32.85	25	20	8	8	303	28.14
11	35	5.5	6	308	36.02	26	20	3	8	313	98.55
12	20	3	4	313	84.35	27	35	5.5	6	308	41.67
13	35	5.5	6	298	29.44	28	20	3	8	303	94.56
14	50	3	8	303	53.90	29	50	3	8	313	58.43
15	50	3	4	303	30.85	30	20	8	8	313	34.14
						31	35	5.5	10	308	98.84

5.1.1. Data analysis and construction of regression model

Regression analysis for adsorption of chromium on nano crystalline zirconia in coded terms of the experimental data yielded the following regression equation:

$$Y = 38.263 - 14.4441\,(\text{initial concentration}) - 21.2035\,(\text{pH}) + 11.7766\,(\text{adsorbent dose}) + 1.5306\,(\text{temperature}) + 4.5452\,(\text{initial concentration})^2 - 1.719\,(\text{pH})^2 + 4.0653\,(\text{adsorbent dose})^2 - 2.5944\,(\text{temperature})^2 + 6.7832\,(\text{initial concentration x pH}) + 0.0149\,(\text{initial concentration x adsorbent dose}) - 0.7306\,(\text{initial concentration x temperature}) - 3.1468\,(\text{pH x adsorbent dose}) - 0.3495\,(\text{pH x temperature}) - 0.1437\,(\text{adsorbent dose x temperature}) \quad (5.1)$$

Here, Y represents the removal (%) of chromium

Regression equation in uncoded terms is expressed as follows:

$$Y = - 9967.31 - 0.3747 \text{ (initial concentration)} - 0.5997 \text{ (pH)} + 1.5613 \text{ (adsorbent dose)} + 64.8128 \text{ (temperature)} + 0.0202 \text{ (initial concentration)}^2 - 0.2750 \text{ (pH)}^2 + 1.0163 \text{ (Adsorbent dose)}^2 - 0.1037 \text{ (temperature)}^2 + 0.1808 \text{ (initial concentration x pH)} + 0.00049 \text{ (initial concentration x adsorbent dose)} - 0.00974 \text{ (initial concentration x temperature)} - 0.6293 \text{ (pH x adsorbent dose)} - 0.02795 \text{ (pH x temperature)} - 0.0143 \text{ (adsorbent dose x temperature)} \quad (5.2)$$

Here, Y also represents the removal (%) of chromium

Table 5.2 Estimated regression coefficients for removal (%) of chromium using nano crystalline zirconia

Term	Coef	SE Coef	p
Constant	38.263	4.024	0.000
Initial concentration	-14.4441	2.173	0.000
pH	-21.2035	2.173	0.000
Adsorbent dose	11.7766	2.173	0.000
Temperature	1.5306	2.173	0.491
Initial concentration*Initial concentration	4.5452	1.991	0.036
pH*pH	-1.719	1.991	0.401
Adsorbent dose*Adsorbent dose	4.0653	1.991	0.058
Temperature*Temperature	-2.5944	1.991	0.211
Initial concentration*pH	6.7832	2.662	0.021
Initial concentration*Adsorbent dose	0.0149	2.662	0.996
Initial concentration*Temperature	-0.7306	2.662	0.787
pH*Adsorbent dose	-3.1468	2.662	0.254
pH*Temperature	-0.3495	2.662	0.897
Adsorbent dose*Temperature	-0.1437	2.662	0.958
S = 10.6467 PRESS = 10256.4			
R-Sq = 92.33% R-Sq(pred) = 56.08% R-Sq(adj) = 85.44 %			

The non significant terms of the model (Equations 5.1 and 5.2) are included in the equation to maintain its hierarchical nature (Zheng *et al.* 2011). The regression coefficient ($R^2 = 92.33$) implies that the equation obtained for adsorption of

chromium on nano crystalline zirconia is valid. The reason for this is that the regression coefficient is more than 80 (Yuliwati *et al.* 2012). ANOVA and regression analysis (Tables 5.2 and 5.3) evaluate significance of variables studied. Initial pH, adsorbent dose and initial concentration were found to be significant among all the variables studied (p value less than 0.05). Additionally, square of initial concentration term, interaction of initial concentration and pH were also found to be significant.

Table 5.3 Analysis of variance for removal (%) of chromium using nano crystalline zirconia

Source	DF	Seq SS	Adj SS	Adj MS	F	p
Regression	14	21539.7	21539.7	1538.6	13.57	0.000
Linear	4	19182.1	19182.1	4795.5	42.31	0.000
Initial concentration	1	5007.2	5007.2	5007.2	44.17	0.000
pH	1	10790.1	10790.1	10790.1	95.19	0.000
Adsorbent dose	1	3328.5	3328.5	3328.5	29.36	0.000
Temperature	1	56.2	56.2	56.2	0.5	0.491
Square	4	1452.2	1452.2	363.1	3.2	0.041
Initial concentration*Initial concentration	1	613.6	590.7	590.7	5.21	0.036
pH*pH	1	101	84.5	84.5	0.75	0.401
Adsorbent dose*Adsorbent dose	1	545.1	472.6	472.6	4.17	0.058
Temperature*Temperature	1	192.5	192.5	192.5	1.7	0.211
Interaction	6	905.5	905.5	150.9	1.33	0.3
Initial concentration*pH	1	736.2	736.2	736.2	6.49	0.021
Initial concentration*Adsorbent dose	1	0	0	0	0	0.996
Initial concentration*Temperature	1	8.5	8.5	8.5	0.08	0.787
pH*Adsorbent dose	1	158.4	158.4	158.4	1.4	0.254
pH*Temperature	1	2	2	2	0.02	0.897
Adsorbent dose*Temperature	1	0.3	0.3	0.3	0	0.958
Residual Error	16	1813.7	1813.7	113.4		
Lack-of-Fit	10	1770.4	1770.4	177	24.56	0.000
Pure Error	6	43.2	43.2	7.2		
Total	30	23353.4				

5.1.2. Effect of initial pH

The strength of the variable is estimated by magnitude of the coefficient. The nature of the variable is estimated by the sign afore to the coefficient. On the basis of these details, pH has the most dominant effect on removal (%) of chromium by

nano crystalline zirconia. The coefficient of initial pH has negative sign afore to its coefficient, it depicts the decrease in removal (%) of chromium with increase of pH (Experimental run '21; 3' and '15; 7' in Table 5.1). Chromium exists as $HCrO_4^-$, $Cr_2O_7^{2-}$and $Cr_4O_{13}^{2-}$ species in the solution (Kiran and Kaushik 2008). The decline in pH of the solution led to surface of adsorbent to be positively charged. The increase in the positive charge on the surface of the adsorbent led to increase in removal (%) of chromium. The fraction of $HCrO^-_4$ increases with increasing pH of solution (Bajpai *et al.* 2012), it depicts the $HCrO_4^-$ has more tendency towards adsorption on nano crystalline zirconia as compared to other species. The high e/m (charge/mass) ratio can be the reason for this as contrast to $Cr_2O_7^{2-}$and $Cr_4O_{13}^{2-}$. The pH_{zpc} of the adsorbent is 6.78 and it depicts that adsorption above this pH is governed by mechanism other than electrostatic attraction. The removal (%) of chromium from aqueous solutions declines more swiftly at lower initial concentration than at higher initial concentration. This is depicted by steeper slope at lower initial concentration than at higher initial concentration (Figure 5.2 A). This could be due to the large difference in removal (%) at lower initial concentration (Experimental run '12; 24' and '3; 21' in Table 5.1) with distinct pH than at higher initial concentration and extreme pH (Experimental run '15; 7' and '10; 19' in Table 5.1).

5.1.3. Effect of initial concentration

Initial concentration was next most dominating factor followed by the pH. The coefficient of the initial concentration has same negative sign afore to its coefficient (Equation 5.1 or 5.2). It depicts that the decline in the removal (%) of chromium with increase of concentration (Figure 5.2 A). The limited number of unsaturated active sites on adsorbent was the reason for aforementioned phenomenon. The numbers of unsaturated sites were more in number at low initial concentration as compared to high initial concentration. On increasing the initial concentration, unsaturated sites become saturated and there will be very few active sites as compared to adsorbate. So, a significant proportion of adsorbate was not able to get adsorbed and remained in the solution. The proportion of nondsorbed species amplifies with increase in initial concentration.

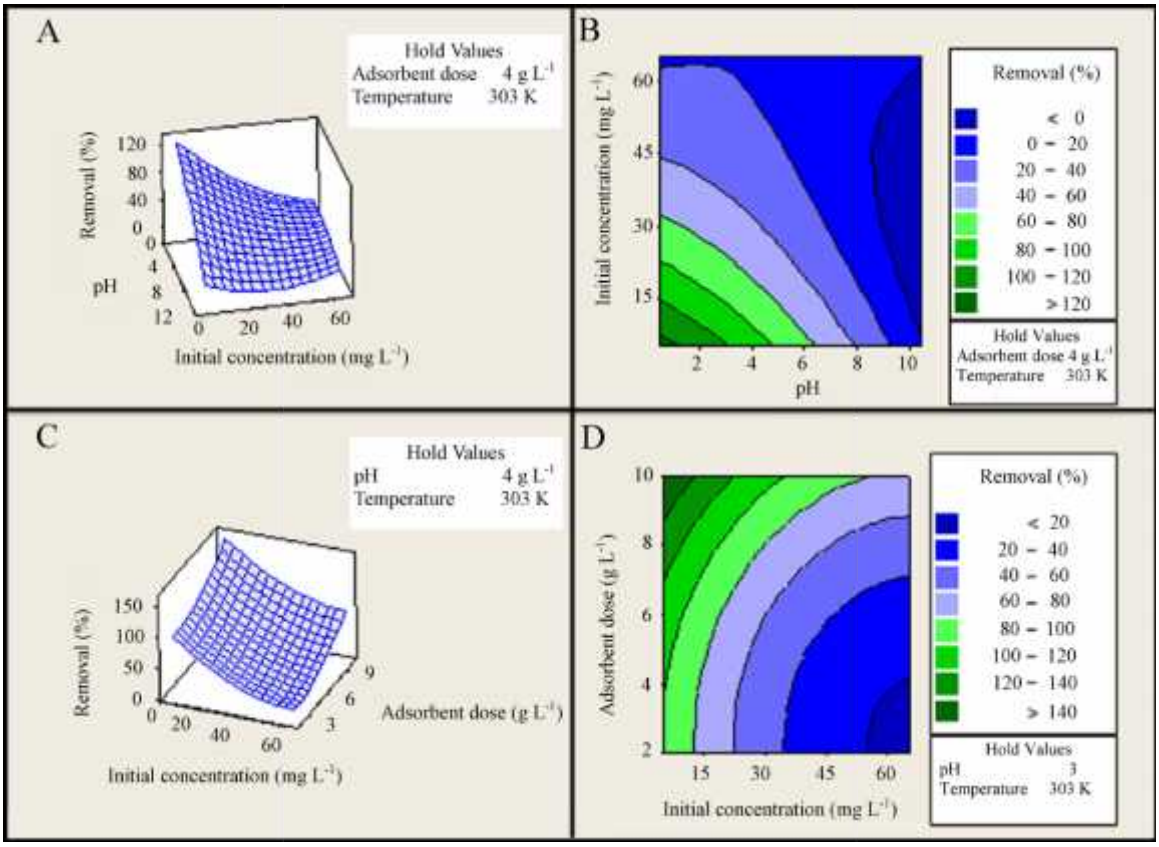

Figure 5.2 A) Surface plot of 'chromium removal (%) *vs.* pH' and initial concentration (mg L^{-1}) at hold values of adsorbent dose and temperature at 4 g L^{-1} and 303K respectively B) Contour plot of 'chromium removal (%) *vs.* pH and initial concentration (mg L^{-1})' at hold values of adsorbent dose and temperature at 4 g L^{-1} and 303K respectively C) Surface plot of 'chromium removal (%) *vs.* adsorbent dose and initial concentration (mg L^{-1})' at hold values of pH and temperature at 3 and 303K respectively D) Contour plot of 'chromium removal (%) *vs.* adsorbent dose and initial concentration (mg L^{-1})' at hold values of pH and temperature at 3 and 303K respectively

5.1.4. Effect of adsorbent dose

Adsorbent dose is third most dominating factor influencing the removal (%) of chromium. The coefficient has positive sign afore to it coefficient; it depicts the chromium removal (%) amplification with increasing adsorbent dose. It can be depicted by comparison of Experimental run '5 and 31' (Table 5.1), where chromium removal (%) increased with increasing adsorbent dose. The reason for aforementioned phenomenon is increase of unsaturated active sites with boost up of adsorbent dose.

5.1.5. Effect of temperature

The temperature has insignificant effect on the removal (%) of chromium (p value more than 0.05). It is also the least dominating parameter affecting removal (%) of chromium from aqueous solutions.

5.1.6. Response surface and contour plots

The response surface and contour plot for chromium removal using nanocrystalline zirconia are represented in Figures 5.2 and 5.3. The Figures 5.2 A, 5.2 B, 5.3A and 5.3B depicts that the removal (%) of chromium decreased with rise of pH.

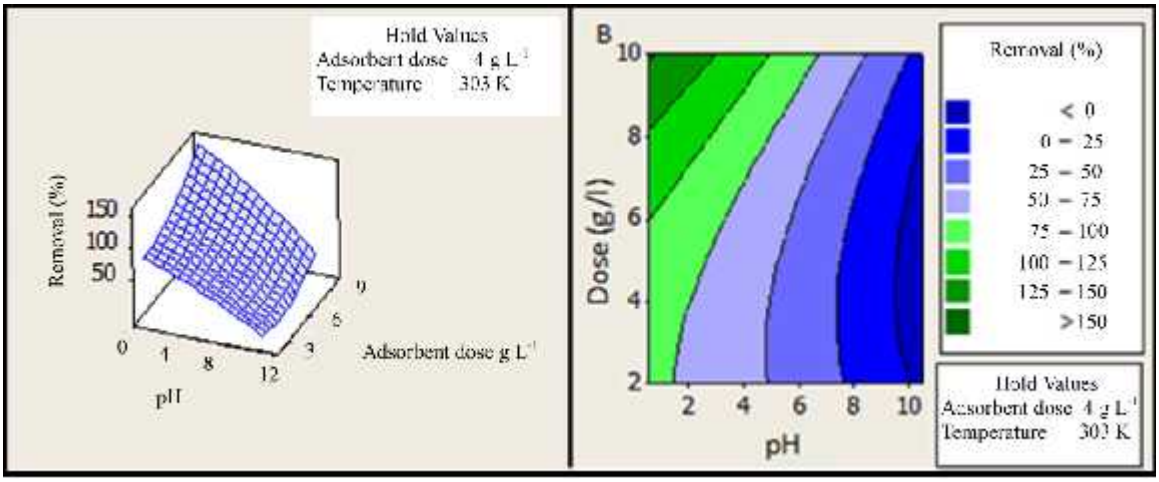

Figure 5.3 A) Surface plot of 'chromium removal (%) *vs.* pH and adsorbent dose' at hold values of initial concentration and temperature at 20 mg L^{-1} and 303K respectively B) Contour plot of 'chromium removal (%) *vs.* pH and dose' at hold values of initial concentration and temperature at 20 mg L^{-1} and 303K respectively

In Figure 5.2 B; the complete removal (%) was depicted below the initial concentration at 15 mg L^{-1} with pH in close proximity to 2. The complete removal was predicted in an area (pH in close proximity to 2 and initial concentration of less than 15 mg L^{-1}) rather than a single point (Hold value of adsorbent dose 4 g L^{-1} and temperature 303 K). Response surface plot (Figure 5.2 C) depicted highest chromium removal (%) at low initial concentration due to larger number of active sites. The lowest removal was obtained at combination of high initial concentration and low adsorbent dose; the phenomenon can be explained by a

smaller amount number of surface active sites for enormous number of adsorbate ions.

The circular nature of the contour plot (Figure 5.2 D) depicts lack of any interaction between adsorbent dose and initial concentration. Figure 5.2 D also depicts the increased removal (%) with increasing adsorbent dose and decreasing initial concentration of chromium. Another response surface plot (Figure 5.3 A) depicts highest removal obtained at high adsorbent dose and low pH. The number of surface active sites amplified in number due to boost up of adsorbent dose and amplification of electrostatic forces of the attraction due to increased surface positive charge; both the factors together raised removal of chromium from aqueous solutions. There was hardly any effect of adsorbent dose predicted above pH 8 up to adsorbent dose of 6 g L^{-1} at hold value of adsorbent dose and temperature at 20 mg L^{-1} and 303 K respectively (Figure 5.3 B).

5.1.7. Optimization of removal (%) of chromium using nano crystalline zirconia

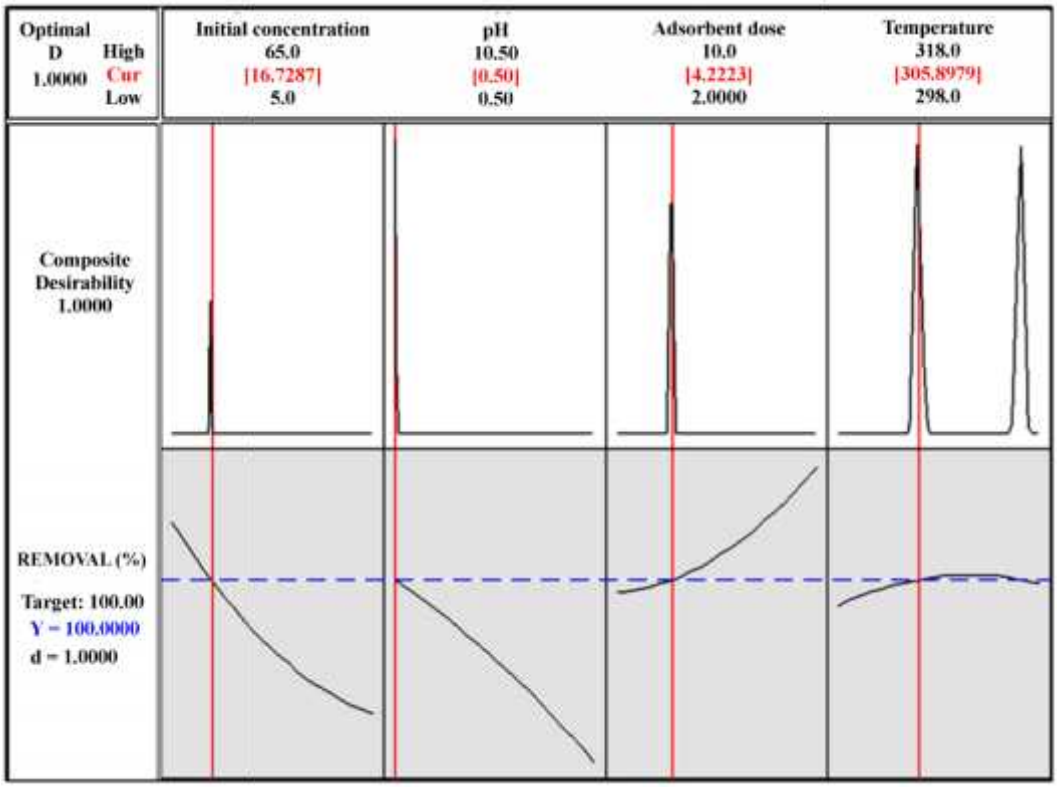

Figure 5.4 Optimization plots for removal of chromium from aqueous solution utilizing nano crystalline zirconia

The optimized results predicted by Minitab 16 software on the basis of RSM results predicted the optimum conditions for removal of chromium as Initial pH = 0.5, Initial chromium concentration = 16.72 mg L^{-1}, Adsorbent dose = 4.22 g L^{-1} and Temperature = 305.8 K (Figure 5.4). Verification of predicted results was done by performing experiment. However, the experimental result is different from the predicted result (Table 5.4). The optimization is achieved by variation of most dominating factor i.e. pH one by one at an interval of 0.5. The results (Table 5.4) depicted that maximum amount of removal (%) of chromium was achieved at pH = 2. So, major removal of chromium occurred at subsequent conditions Initial pH = 2.0, Initial chromium concentration = 16.72 mg L^{-1}, Adsorbent dose = 4.22 g L^{-1}, Temperature = 305.8 K.

Table 5.4 Experiments at variable pH with optimum initial concentration and adsorbent dose

S.No.	pH	Removal (%)
1	0.5	41.89
2	1	53.64
3	1.5	70.19
4	2.0	99.85
5	2.5	92.26

5.2. Linear approach for isotherm analysis

The isotherm parameters determined by linear analysis are displayed in Table 5.5. The graph by linear curve fitting is plotted and represented as Figures 5.5 and 5.6. The linear Langmuir isotherm plot (Figure 5.5) showed the predicted data is proximate to experimental data. The linear Freundlich isotherm plot also (Figure 5.6) depicts the close proximity of experimental and predicted data. However, experimental data points in some cases in Freundlich isotherm plot (Figure 5.6) are far from the predicted data. The plots (Figures 5.5 and 5.6) cannot be able to clearly differentiate the best suitable isotherm model. The Langmuir constants Q_o and b were estimated from the slopes and intercepts of 'C_e/q_e *vs.* C_e' plot (Figure 5.5) respectively. The increase in value of Q_o with temperature portrays increased maximum adsorption capacity with rise of temperature. The endothermic nature of

adsorption process is depicted by increase of value of Q_o with temperature. Similarly, Freundlich isotherm parameters K_F and 1/n were calculated from the intercepts and slopes of plot '$\log q_e$ *vs.* $\log C_e$' (Figure 5.6).

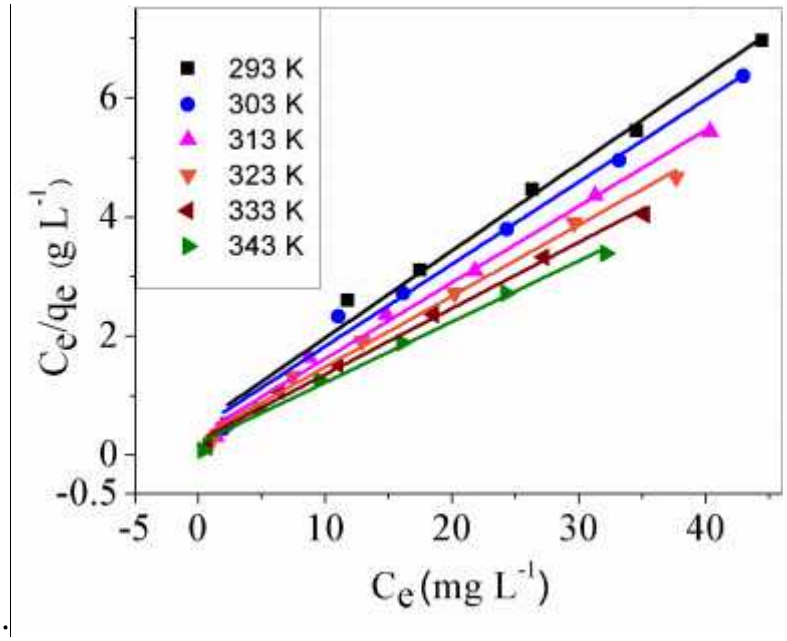

Figure 5.5 Linear Langmuir isotherm plot of chromium removal using nano crystalline zirconia (dots represent the experimental data and lines represent the data estimated by the model)

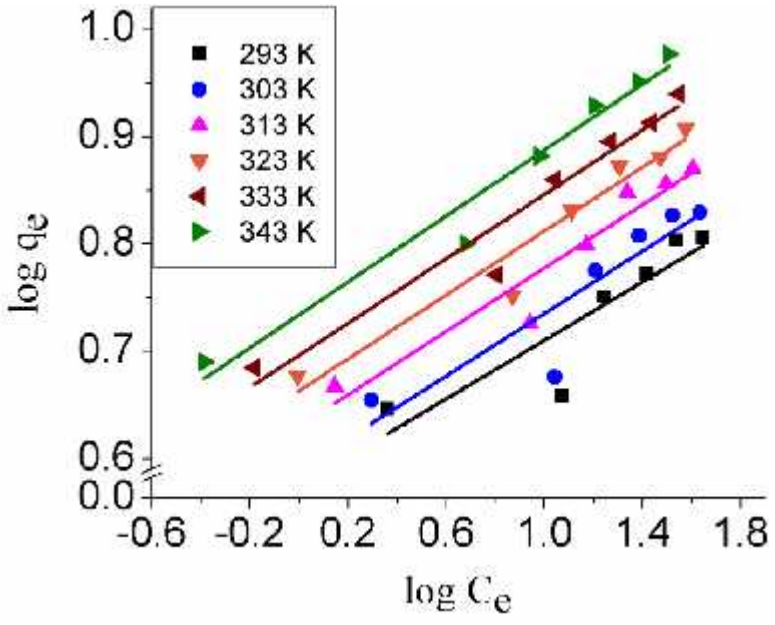

Figure 5.6 Linear Freundlich isotherm plot of chromium removal using nano crystalline zirconia (dots represent the experimental data and lines represent the data estimated by the model)

Table 5.5 Langmuir and Freundlich isotherm parameters for linear analysis and nonlinear analysis by Microcal origin for adsorption of chromium from aqueous solution on nano crystalline zirconia

Analysis method	**Temp.**	**Langmuir parameters**			**Freundlich parameters**		
	(K)	**Q_o (mg/g)**	**b(L/mg)**	**R^2_{adj}**	**K_F(mg/g)(L/mg)$^{1/n}$**	**1/n**	**R^2_{adj}**
Linear	293	6.82	0.2913	0.9872	3.7452	0.1364	0.7568
	303	7.23	0.3121	0.9875	3.8834	0.1456	0.7767
	313	7.80	0.3811	0.9927	4.2623	0.1476	0.9031
	323	8.37	0.4184	0.9921	4.6007	0.1488	0.9298
	333	9.01	0.452	0.9916	4.9638	0.1501	0.9313
	343	9.68	0.4774	0.9920	5.4147	0.1537	0.9585
Microcal origin							
	293	6.11	0.9044	0.4844	3.6345	0.1474	0.7928
	303	6.50	0.9146	0.5212	3.7790	0.1560	0.8076
	313	7.04	1.1358	0.6297	4.1726	0.1558	0.9121
	323	7.47	1.4569	0.6438	4.5072	0.1570	0.9368
	333	7.91	1.9807	0.6229	4.8519	0.1597	0.9400
	343	8.49	2.7321	0.6265	5.2896	0.1640	0.9646

The values of coefficient of determination were higher for Langmuir isotherm as compared to that for Freundlich isotherm. Hence, the isotherm data fit better in Langmuir isotherm model than Freundlich isotherm model. Value of K_F increased with increase in temperature suggesting endothermic nature of adsorption process. Another constant n is a yardstick of adsorption intensity or surface heterogeneity. As the value of n increases (or 1/n approaches decreases), the surface heterogeneity is escalated. In the present case, value of 1/n increases hence abatement of surface heterogeneity occurred with increase in temperature. On comparison of R^2_{adj} of both the isotherms models (Table 5.5), it has been concluded that chromium adsorption on nano crystalline zirconia is better interpreted by Langmuir isotherm.

5.3. Nonlinear approach for isotherm analysis

Nonlinear analysis was performed as linear regression is marred by change of error structure, violation of error variance due to transformation of native equation into linear equation (Foo and Hameed 2010). Nonlinear analysis was performed using error analysis by solver add-in of Microsoft excel and customized curve fitting function of Microcal origin. The estimated isotherm parameters are

displayed in Tables 5.5 and 5.6. The data is represented in graphical form in Figure 5.7 to Figure 5.10. The nonlinear Freundlich isotherm plot (Figure 5.7) depicts the vast difference between the experimental data and data predicted by error analysis method.

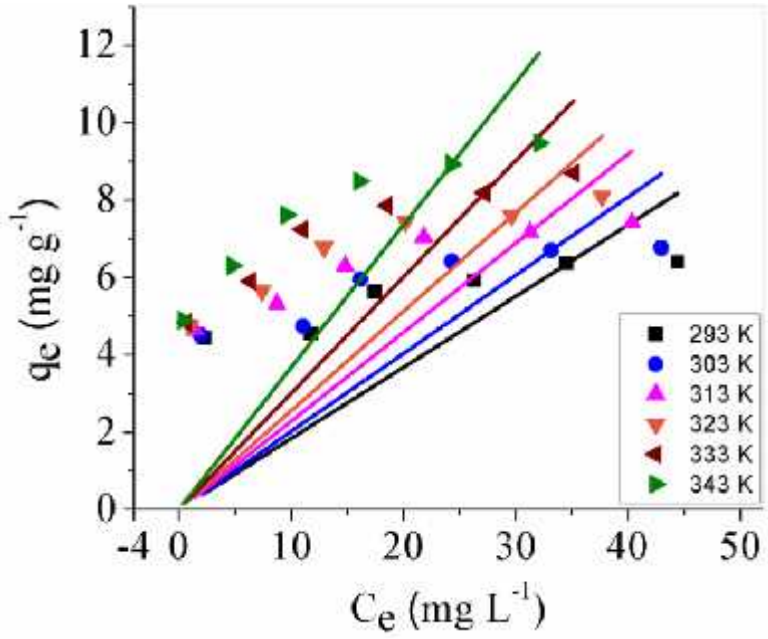

Figure 5.7 Nonlinear Freundlich isotherm plot of chromium removal using nano crystalline zirconia obtained by error analysis method (dots represent the experimental data and lines represent the data estimated by the model)

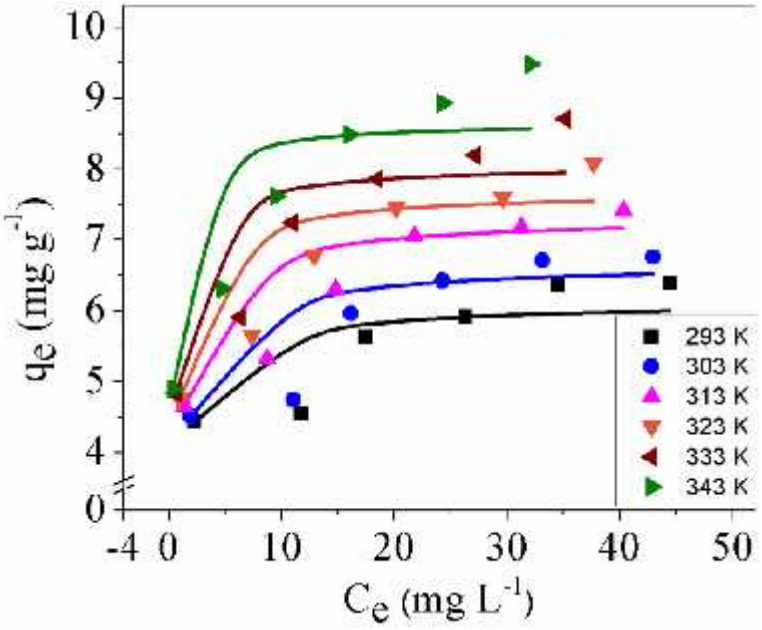

Figure 5.8 Nonlinear Langmuir isotherm plot of chromium removal using nano crystalline zirconia obtained by error analysis method (dots represent

the experimental data and lines represent the data estimated by the model)

The data predicted by error analysis method depicted in Langmuir isotherm plot (Figure 5.8) is closer to experimental data than in Freundlich isotherm plot (Figure 5.7). However, the data predicted by error analysis method in Langmuir isotherm plot (Figure 5.8) is also not proximate to experimental data. In error analysis, the system with least normalized sum of error is selected as optimum error function and its parameters were used for comparison and further study. Error function analysis of Langmuir isotherm depicted that four systems are better explained by MPSD and two systems by ARE.

Table 5.6 Langmuir and Freundlich isotherm parameters by error analysis method for adsorption of chromium from aqueous solution on nano crystalline zirconia

	Langmuir parameters				**Freundlich parameters**			
Temp.	**Error function**	**Q_o (mg/g)**	**b (L/mg)**	**R^2_{adj}**	**Error function**	**K_F $(mg/g)(L/mg)^{1/n}$**	**1/n**	**R^2_{adj}**
293K	MPSD	6.1121	1.1368	0.2705	ARE	0.3826	0.4804	-13.1033
303K	MPSD	6.6577	1.0600	0.2658	EABS	0.3986	0.5070	-11.3079
313K	MPSD	7.3044	1.2519	0.3725	ARE	0.3492	0.6572	-11.1582
323K	ARE	7.6703	1.6494	0.4529	EABS	0.3889	0.6587	-10.0183
333K	MPSD	8.0445	2.2877	0.4597	ARE	0.4348	0.6912	-8.399
343K	ARE	8.6539	3.1671	0.4648	ARE	0.5284	0.6958	-6.9962

Similarly, in Freundlich isotherm, four systems are explained by ARE and two systems by EABS. The coefficient of determination was superior for Langmuir isotherm as compared to Freundlich isotherm (Table 5.6). The above mentioned reasons explained the suitability of Langmuir isotherm model on experimental data.

Nonlinear analysis was also performed using customized curve fitting function of Microcal origin. The nonlinear Langmuir isotherm plot (Figure 5.9) depicts the difference between the experimental data and data predicted by customized Microcal origin function. However, the data predicted by customized Microcal

origin function depicted in Freundlich isotherm plot (Figure 5.10) is closer to experimental data than in Langmuir isotherm plot (Figure 5.9).

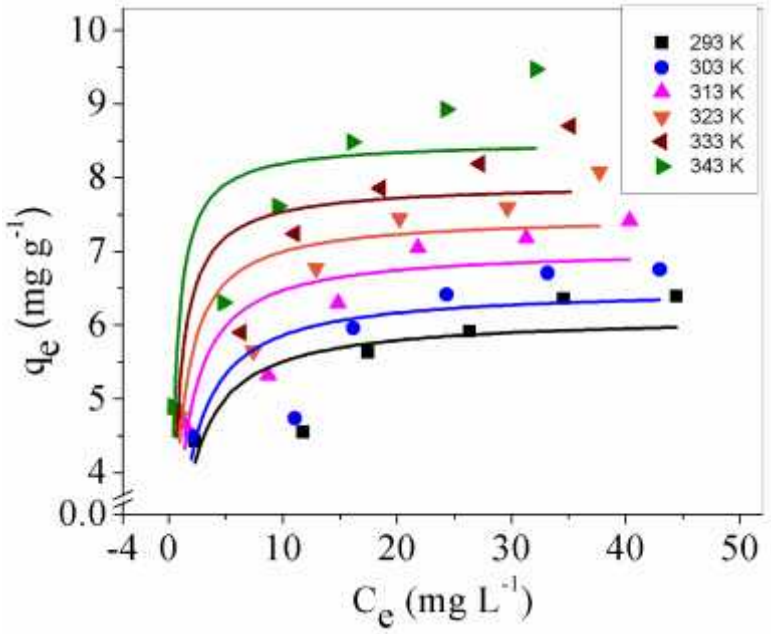

Figure 5.9 Nonlinear Langmuir isotherm plot of chromium removal using nano crystalline zirconia obtained by customized Microcal origin function (dots represent the experimental data and lines represent the data estimated by the model)

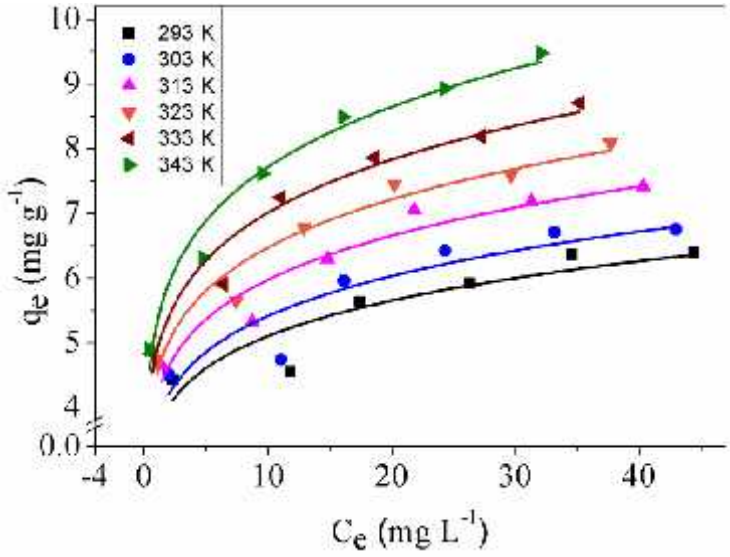

Figure 5.10 Nonlinear Freundlich isotherm plot of chromium removal using nano crystalline zirconia obtained by customized Microcal origin function (dots represent the experimental data and lines represent the data estimated by the model)

The comparison between plots (Figures 5.9 and 5.10) suggest the suitability of Freundlich isotherm model. The coefficients of determination for Langmuir isotherm model were lower than that for Freundlich isotherm model using customized curve fitting function of Microcal origin (Table 5.5). Hence, it predicted the suitability of Freundlich isotherm model. However, linear method suggests superiority of Langmuir isotherm model in fitting isotherm data. So, linear analysis is preferred due to high coefficient of determination.

5.4. Linear approach for kinetic model analysis

The linear pseudo-first order plot (Figure 5.11) showed the predicted data is proximate to most of the experimental data except at few data points. The linear pseudo-second order plot also (Figure 5.12) depicts the close proximity of experimental and predicted data. However, the data predicted for pseudo-second order in the plot (Figure 5.12) depicts more proximity of experimental data to predicted data than depicted by pseudo-first order plot (Figure 5.11). The parameters obtained from linear analysis of kinetic data (Figure 5.11 and 5.12) are represented in Table 5.7 along with coefficient of determination. The pseudo-second order model fits the data better as compared to pseudo-first order model.

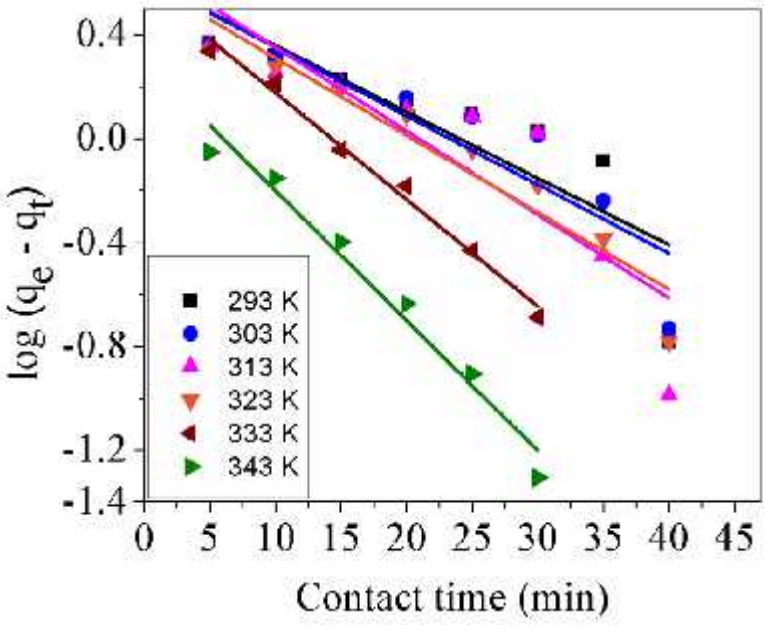

Figure 5.11 Linear pseudo-first order plot of chromium removal using nano crystalline zirconia (dots represent the experimental data and lines represent the data estimated by the model)

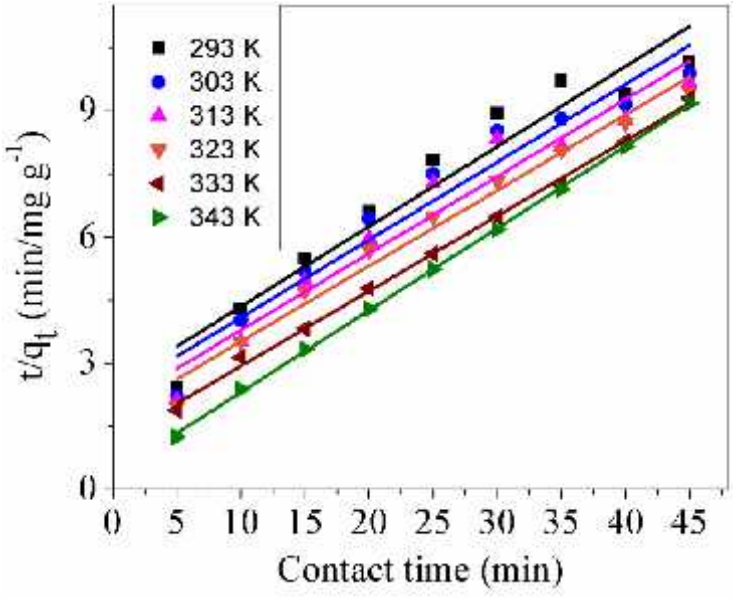

Figure 5.12 Linear pseudo-second order plot of chromium removal using nano crystalline zirconia (dots represent the experimental data and lines represent the data estimated by the model)

Table 5.7 Pseudo-first order and pseudo-second order kinetic parameters for linear analysis and nonlinear analysis by Microcal origin for adsorption of chromium from aqueous solution on nano crystalline zirconia

			Pseudo-first order			**Pseudo-second order**		
Analysis method	**Temp. (K)**	**Experimental q_e (mg/g)**	**q_e (mg/g)**	**k_1 (min^{-1})**	**R^2_{adj}**	**q_e (mg/g)**	**k_2 ($g.mg^{-1}min^{-1}$)**	**R^2_{adj}**
Linear	293	4.4237	4.0633	0.0585	0.6898	5.2499	0.01483	0.9264
	303	4.5472	4.5571	0.0698	0.7906	5.4054	0.01529	0.9338
	313	4.6501	4.7402	0.0743	0.7325	5.4648	0.01713	0.9412
	323	4.7531	4.1607	0.0712	0.8938	5.5568	0.01887	0.9796
	333	4.8353	3.8872	0.0949	0.9863	5.7065	0.02556	0.9905
	343	4.9022	1.1501	0.1039	0.9787	5.1509	0.10084	0.9997
Microcal origin	293	4.4237	4.0707	0.0802	0.7225	3.2212	1.3E+45	-0.1429
	303	4.5472	3.3857	59.7746	-0.1429	3.3858	1.2E+44	-0.1429
	313	4.6501	3.5704	26.8679	-0.1429	3.5704	2.4E+45	-0.1429
	323	4.7531	3.7469	38692.91	-0.1429	3.7468	-2E+44	-0.1429
	333	4.8353	3.9828	71166.86	-0.2000	3.9828	-2.1E+45	-0.2000

	343	4.9022	4.5594	20.7662	-0.2000	4.5594	1.7E+45	-0.2000

The theoretical q_e values retrieved from pseudo-second order model were closer to experimental values as compared with theoretical q_e values computed from pseudo-first order model. In addition to this, the value of coefficient of determination was higher for pseudo-second order model. Hence, the system follows pseudo-second order model.

5.5. Nonlinear analysis of kinetic data

Kinetic model parameters determined by nonlinear analysis (Figures 5.13 to 5.16) of kinetic data are displayed in Tables 5.7 and 5.8. The nonlinear pseudo-first order plot (Figure 5.13) and pseudo-second order plot (Figure 5.14) depicts the vast difference between the experimental data and data predicted by customized Microcal origin function. The customized Microcal origin function method cannot be able to predict the kinetic parameters as depicted by Figures 5.13 and 5.14.

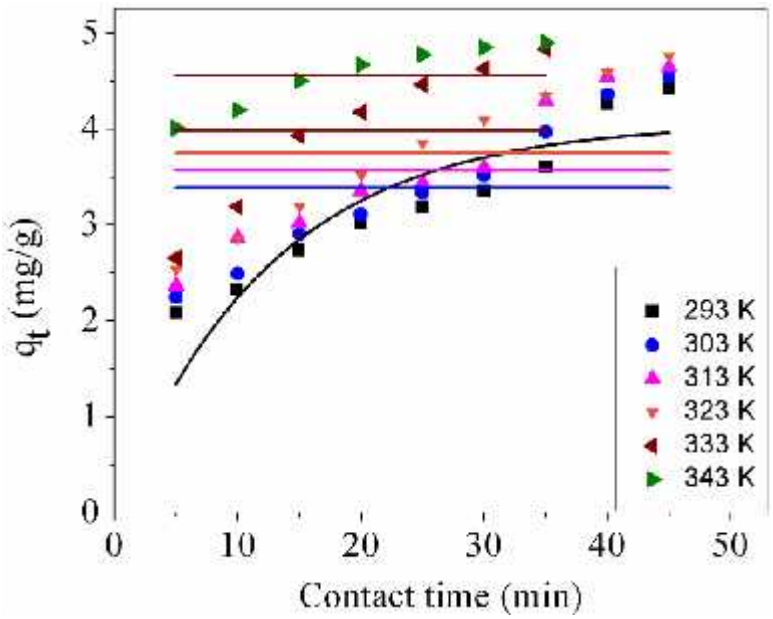

Figure 5.13 Nonlinear pseudo-first order plot of chromium removal using nano crystalline zirconia obtained by customized Microcal origin function (dots represent the experimental data and lines represent the data estimated by the model)

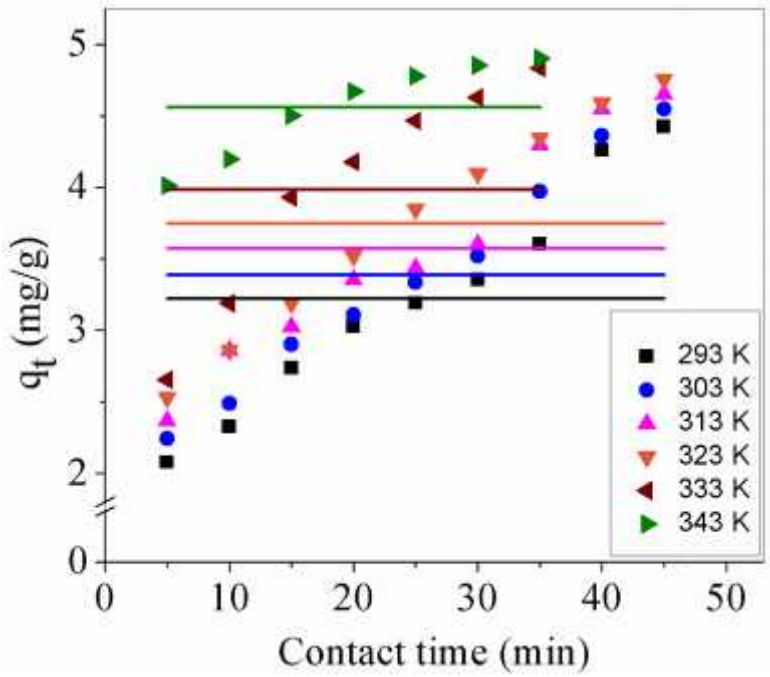

Figure 5.14 Nonlinear pseudo-second order plot of chromium removal using nano crystalline zirconia obtained by customized Microcal origin function (dots represent the experimental data and lines represent the data estimated by the model)

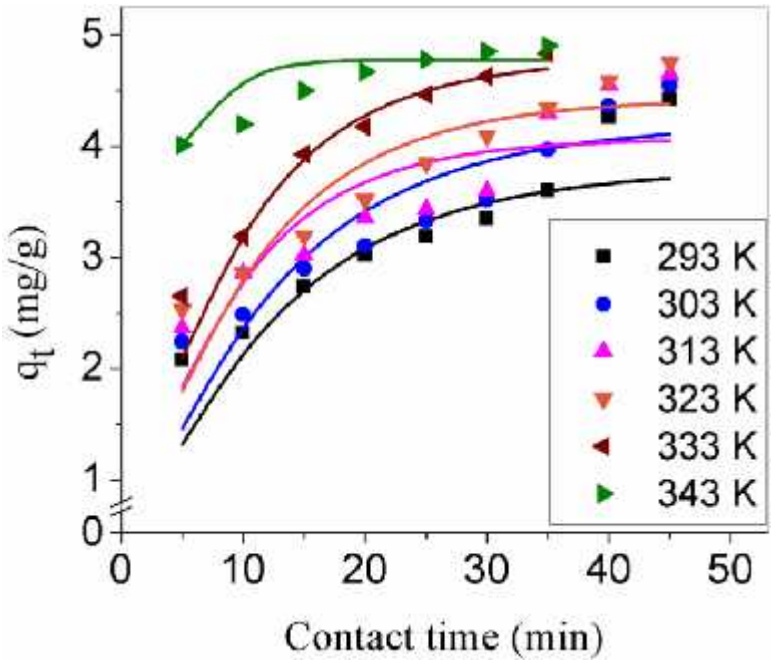

Figure 5.15 Nonlinear pseudo-first order plot of chromium removal using nano crystalline zirconia obtained by error analysis function (dots represent the experimental data and lines represent the data estimated by the model)

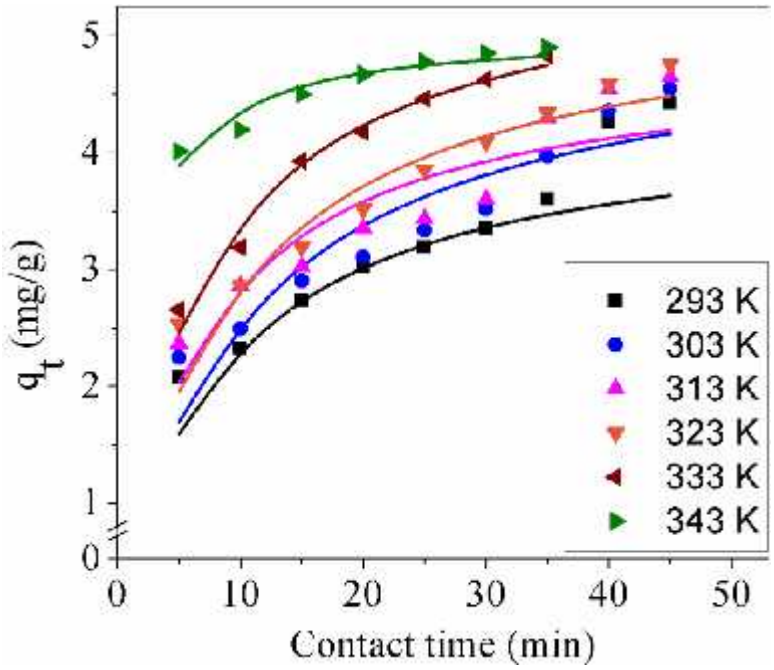

Figure 5.16 Nonlinear pseudo-second order plot of chromium removal using nano crystalline zirconia obtained by error analysis function (dots represent the experimental data and lines represent the data estimated by the model)

The nonlinear pseudo-first plot (Figure 5.15) depicts the close proximity between the experimental data and data predicted by error analysis method. Similarly, nonlinear pseudo-second order plot (Figure 5.16) also depicts the close proximity between the experimental data and data predicted by error analysis method. The two plots (Figures 5.15 and 5.16) cannot be able to differentiate the suitability of the better kinetic model.

Table 5.8 Pseudo-first order and pseudo-second order model constants by error analysis method for adsorption of chromium from aqueous solution on nano crystalline zirconia

	Pseudo-first order				Pseudo-second order			
Temp. (K)	**Error function**	**k_1 (min^{-1})**	**q_e (mg/g)**	**R^2_{adj}**	**Error function**	**k_2 ($g.mg^{-1}min^{-1}$)**	**q_e (mg/g)**	**R^2_{adj}**
293	EABS	0.0852	3.7930	0.6025	MPSD	0.0268	4.3269	0.6754
303	ERRSQ	0.0855	4.1974	0.6612	ERRSQ	0.0195	5.0968	0.8071
313	HYBRID	0.1202	4.0670	0.5177	HYBRID	0.0299	4.8362	0.7726
323	ERRSQ	0.1040	4.4274	0.7153	ARE	0.0214	5.3552	0.8639
333	MPSD	0.1150	4.7826	0.8740	EABS	0.0275	5.6245	0.9676
343	EABS	0.3668	4.7752	0.4180	ERRSQ	0.1362	5.0273	0.9994

In Error analysis method, the function with least normalized sum of error is selected. In pseudo-first order model; out of six systems, two systems each are explained by ERRSQ and EABS. One system is explained each by HYBRID and MPSD. Similarly, in pseudo-second order model, two systems have least normalized sum of error for ERRSQ. One system each is explained better by EABS, ARE, HYBRID and MPSD. The pseudo-second order model has larger coefficient of determination as compared to that with pseudo-first order model (Table 5.8). Hence, in this case, the system follows pseudo-second order model.

On the basis of linear and nonlinear analysis, pseudo-second order model succeeded as the preferable model for explaining the kinetic data. Kinetic parameters obtained by linear analysis were succeeded to explain the kinetics of adsorption of chromium on nano crystalline zirconia on the basis of high coefficient of determination.

5.6. Intraparticle diffusion model

The kinetic data was fitted into intraparticle diffusion model suggested by Weber and Morris (Weber and Morris 1963). Intraparticle diffusion graph plotted between q_t and $t^{1/2}$ is shown in Figure 5.17. The k_{diff}, C_b and R^2_{adj} are shown in Table 5.9. The intercept (C_b) depicts the thickness of boundary layer. The bigger the value of intercept, bigger is the boundary layer.

Table 5.9 Intraparticle diffusion parameters for adsorption of chromium from aqueous solution on nano crystalline zirconia

S.No.	Temperature (K)	K_{diff} (mg/g $min^{1/2}$)	C_b (mg g^{-1})	R^2_{adj}
1	293	0.4833	1.0417	0.9607
2	303	0.4631	1.316	0.9427
3	313	0.4533	1.5277	0.9659
4	323	0.3879	2.2236	0.8357
5	333	0.1605	3.8271	0.8143
6	343	0.4881	0.8610	0.9559

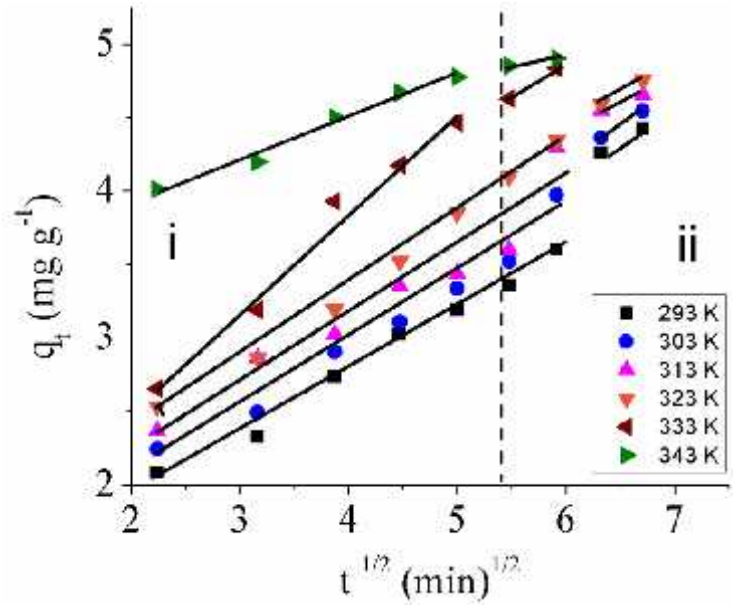

Figure 5.17 Intraparticle diffusion plot for removal of chromium from aqueous solution utilizing nano crystalline zirconia

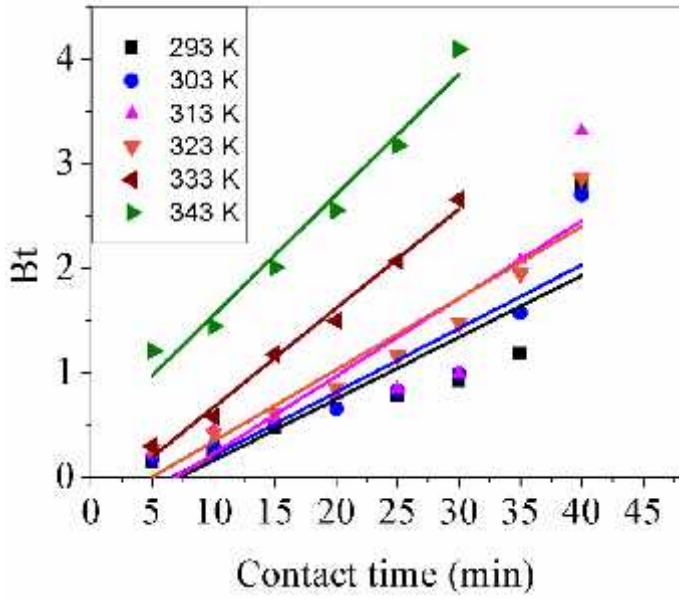

Figure 5.18 Boyd model plot for removal of chromium from aqueous using nano crystalline zirconia

There were two regions in intraparticle diffusion plot. It depicts time dependent adsorption process. Initially, the rate of chromium uptake was faster and afterwards it slowed down with time. The slopes of first and second level show deviation from origin. The deviation of slope from origin is attributed to the difference in the mass transfer rate of initial and final stages of adsorption. It validates the existence of boundary layer diffusion as rate limiting step for adsorption of chromium by nanocrystalline zirconia (Mohanty *et al.* 2005).

To further investigate the actual slow step of adsorption process; kinetic data is further analyzed with Boyd model simplified by Reichenberg (Boyd *et al.* 1947;Reichenberg 1953). Boyd model differentiates adsorption rate controlling step between boundary layer and particle diffusion: diffusion inside the pores. Boyd plot is represented by graph 'Bt *vs.* t' (Figure 5.18). In the present case, graph (Figure 5.18) did not pass from the origin which means that the process of removal is not controlled by adsorption only, it administrated by boundary layer diffusion mechanism also.

5.7. Thermodynamic study

5.7.1. Determination of thermodynamic parameters using Langmuir constant method

Thermodynamic parameters i.e. change in standard free energy change (ΔG^o), change in standard enthalpy (ΔH^o) and change in standard entropy (ΔS^o) were estimated using following well known equations (Gupta and Rastogi 2009;Liu 2009;Salvestrini *et al.* 2014):

$$\Delta G_o = -RT\ln K_L \tag{5.3}$$

$$\ln K_L = \frac{\Delta S_o}{R} - \frac{\Delta H_o}{RT} \tag{5.4}$$

Langmuir constant b is used to calculate thermodynamic equilibrium constant i.e. K_L (L mol^{-1}) (Liu 2009), and R is gas constant (8.314 J $mol^{-1}K^{-1}$). The ΔH^o and ΔS^o were calculated from the slope and intercept of plot between $\ln K_L$ and 1/T respectively (Elkady *et al.* 2011). The K_L is estimated from the following equation:

$$K_L = \frac{b}{\gamma_e} \tag{5.5}$$

$$\log\gamma_e = -A_1 z^2 I_e^{1/2} \tag{5.6}$$

Here γ_e is the activity coefficient, I_e is the ionic strength (1.1 x 10^{-3} mol/kg) of the

solute at equilibrium, A_1 is a constant (0.509 $mol^{-1/2}$ $kg^{1/2}$) and z is the charge on ion. The calculated values of the parameters ΔG^o, ΔH^o and ΔS^o parameters are presented in the Table 5.10.

Thermodynamic parameters estimated utilizing linear and nonlinear equation parameter (b) by Langmuir constant method depict slight variation in magnitude for change in free energy and change in entropy. It is estimated that the adsorption process was spontaneous, endothermic and occurred with increase in entropy.

Table 5.10 Thermodynamic parameters estimated by Langmuir constant method for adsorption of chromium by nano crystalline zirconia

Parameter	Equation	Temp. (K)	Parameters using linear equation parameter b	Parameters using nonlinear equation parameter b (Error)	Parameters using nonlinear equation parameter b (Microcal origin)
ΔG^o (kJ mol^{-1})	$\Delta G^o = -RT \ln K_L$	293	-23.7908	-27.1077	-26.5507
		303	-24.7765	-27.8567	-27.4852
		313	-26.114	-29.2091	-28.9558
		323	-27.199	-30.8818	-30.5495
		333	-28.255	-32.7446	-32.3456
		343	-29.2594	-34.6554	-34.2341
ΔH^o (kJ mol^{-1})	$\ln K_L = \frac{\Delta S^o}{R} - \frac{\Delta H^o}{RT}$		8.8185	18.121	19.112
ΔS^o (kJ $mol^{-1}K^{-1}$)			0.1112	0.1520	0.1545
R^2_{adj}			0.9643	0.8431	0.9118

The thermodynamic equilibrium constant determined by linear analysis method was used to calculate thermodynamic parameters. The high R^2_{adj} for linear analysis (0.9643) suggested use of this model.The positive value of enthalpy change (ΔH^o = 8.818 kJ mol^{-1}) supported the endothermic nature of adsorption process. The ΔG^o value becomes more negative on raising temperature. It depicts the feasibility of the process is more at higher temperature. The positive value of entropy change (0.1112 kJ mol^{-1}) recommends the increase of disorderness at adsorbent and adsorbate surface.

5.7.2. Determination of thermodynamic parameters using partition method

In partition method, the distribution coefficient, K_p or K_c were used in place of K_L (Liu 2009;Salvestrini *et al.* 2014):

$$K_P \text{ or } K_C = \frac{C_S}{C_W} \tag{5.7}$$

Table 5.11 Thermodynamic parameters calculated by partition method for adsorption of chromium by nano crystalline zirconia

Temp. (K)	ΔG^o (kJ mol^{-1})	ΔH^o (kJ mol^{-1})	ΔS^o (kJ mol^{-1} K^{-1})	R^2_{adj}	ΔG^o (kJ mol^{-1})
	$\Delta G^o = -RT \ln K^P$	$\ln K^P = \frac{\Delta S^o}{R} - \frac{\Delta H^o}{RT}$			$\Delta G^o = \Delta H^o - T\Delta S^o$
293	-4.9651	30.752	0.1208	0.95995	-4.6414
303	-5.8115				-5.8494
313	-6.7324				-7.0574
323	-7.9417				-8.2654
333	-9.3576				-9.4733
343	-11.1644				-10.6814

Here C_s and C_w represent the concentration of adsorbate in solid and liquid phase. Afterwards, Equations 5.3 and 5.4 were used for determination of thermodynamic parameters. In addition to this, the change in free energy was computed from the following equation (Salvestrini *et al.* 2014):

$$\Delta G_o = \Delta H_o - T\Delta S_o \tag{5.8}$$

The estimated values of thermodynamic parameters ΔG^o, ΔH^o and ΔS^o by partitioned method are provided in Table 5.11. The endothermic nature of adsorption is indicated by positive values of enthalpy change (ΔH^o = 30.75 kJ mol^{-1}). Similarly, the values of free energy change (ΔG^o) were negative and it recommended that the process of removal of chromium was spontaneous in nature. The values of ΔG^o calculated from equation 5.8 were also negative recommending the spontaneous nature of adsorption. The positive estimations from ΔS^o predicted

the increase of disorderness at adsorbate and adsorbent surface during the process of adsorption. However, K_c or K_p is equivalent to thermodynamic equilibrium constant (K_L) at lower concentration (Liu 2009). So, thermodynamic parameters estimated by Langmuir constant method are preferred over partition method.

5.7.3. Activation Energy

Arrhenius equation is used to determine activation energy of adsorption process (Arrhenius 1889). It depicts the minimum energy required for feasibility of adsorption to occur. The equation of activation energy is represented as follows (Chen *et al.* 2013):

$$\ln k_2 = \ln A - E_a/RT \quad (5.9)$$

Here k_2 (g mg $^{-1}$ min^{-1}) represents the rate constant obtained from the pseudo-second order kinetic model, E_a (J mol^{-1}) is the Arrhenius activation energy of adsorption and A is the Arrhenius factor. The slope of $-E_a/R$ is obtained by a plot between '$\ln k_2$ *vs.* 1/T'. The activation energy calculated is 10.39 kJ mol^{-1}, which is adequate.

5.8. Desorption experiments

Three desorbing agents NaOH, KOH and NH_4OH (0.1N) were used to desorb the adsorbed chromium from the adsorbent. NaOH, KOH and NH_4OH (0.1N) solutions showed desorption efficiency of 74.85 %, 74.85 % and 84.53 % respectively (Table 5.12).

Table 5.12 Desorption efficiency of 0.1N NaOH, 0.1N KOH, 0.1N NH_4OH for chromium loaded nano crystalline zirconia

S.No.	Desorbing agent	Desorption efficiency
1	0.1 N NaOH	74.85
2	0.1N KOH	74.85
3	0.1N NH_4OH	84.53

NH_4OH 0.1 N solution has shown best results for desorption and it is reused up to three cycles for the removal of chromium, after third cycle desorption efficiency is reduced drastically (Table 5.13).

Table 5.13 Chromium removal (%) after subsequent regeneration cycle (Initial concentration =20 mg L^{-1}, pH = 2, Adsorbent dose = 4 g L^{-1}, Temperature = 303 K)

S.No.	Regeneration cycle	Chromium removal (%) after regeneration cycle
1	1^{st}	96.37
2	2^{nd}	95.39
3	3^{rd}	91.76
4	4^{th}	62.45

It would be noteworthy that the adsorbent could be used successfully without much loss of capacity for three runs and thus reducing cost of treatment.

5.9. Conclusions

Chromium was effectively removed from aqueous solutions using nanocrystalline zirconia as an adsorbent. The adsorption equilibrium time was 45 min. The pH was most dominating factor for removal of chromium using nano crystalline zirconia. The most dominant factor pH was followed by factors i.e. initial concentration and adsorbent dose affecting adsorption of chromium. However, temperature did not significantly affect the removal of chromium from aqueous solutions. Optimum parameters were initial concentration, pH, adsorbent dose and temperature at 16.72 mg L^{-1}, 2, 4.22 g L^{-1} and 305.8 K respectively. The isotherm and kinetic models data fitted better with linear curve fitting analysis. The data for chromium removal by nanocrystalline zirconia follows Langmuir isotherm model and pseudo-second order kinetic model. The change in Gibbs free energy was negative showing spontaneous nature of the adsorption process. The adsorption of chromium using nanocrystalline zirconia was endothermic in nature and occurred with increase of entropy. The regeneration of the adsorbent was done with ammonium hydroxide and showed steady results up to three regeneration cycles.